

# Biodegradation Behavior of Cellulose Acetate with DS 2.5 in Simulated Soil

Roberta Ranielle M. de Freitas, Vagner R. Botaro

**Abstract**—The relationship between biodegradation and mechanical behavior is fundamental for studies of the application of cellulose acetate films as a possible material for biodegradable packaging. In this work, the biodegradation of cellulose acetate (CA) with DS 2.5 was analyzed in simulated soil. CA films were prepared by casting and buried in the simulated soil. Samples were taken monthly and analyzed, the total time of biodegradation was 6 months. To characterize the biodegradable CA, the DMA technique was employed. The main result showed that the time of exposure to the simulated soil affects the mechanical properties of the films and the values of crystallinity. By DMA analysis, it was possible to conclude that as the CA is biodegraded, its mechanical properties were altered, for example, storage modulus has increased with biodegradation and the modulus of loss has decreased. Analyses of DSC, XRD, and FTIR were also carried out to characterize the biodegradation of CA, which corroborated with the results of DMA. The observation of the carbonyl band by FTIR and crystalline indices obtained by XRD were important to evaluate the degradation of CA during the exposure time.

**Keywords**—Biodegradation, cellulose acetate, DMA, simulated soil.

## I. INTRODUCTION

THE search for materials from renewable sources has been increasing year after year in an attempt to substitute raw materials from non-renewable sources and which are biodegradable, with durability in use and biodegradation at disposal [1], [2]. Biodegradable polymers are those that, when in the presence of microorganisms, undergo degradation. Biodegradable polymers can be derived from renewable natural sources, e.g. maize, cellulose, potato, or sugarcane are synthesized by bacteria. Most interesting are polymers from renewable sources, since they form a closed life cycle [3]. Main cellulose derivative is CA [4], which is mainly used in membranes, films, fibers, filters, as a component in adhesives and pharmaceuticals [5]. As cellulose is biodegradable in the presence of the enzyme cellulase, the same is expected for CA. [6], [7]. This work had the objective of analyzing the biodegradability of the CA, in simulated soil, and its dynamic-mechanical thermal behavior. FTIR, DSC, and DRX techniques were used to complement and confirm the results obtained in the DMA.

## II. EXPERIMENTAL

In the biodegradation test, simulated soil with equine manure was used. The following mass percentages were used; 23% manure, 23% sand, 23% soil and 31% water [7]. The CA,

supplied by the Rhodia Sovay® group, with a degree of substitution of 2.5, was solubilized in acetone in the proportion of 10% (m/v). After solubilization, they were added to the petri dish, capped, and kept at room temperature. After the samples were obtained by casting, they were cut in approximate measurements (length/width/thickness) equal to: 10/7/0.5 mm. Samples of CA films, with DS 2.5, in triplicate, were buried in the simulated soil and stored in isolated light and at room temperature. From 0 to 6 months, samples were collected, washed with demineralized water, dried and weighed. DMA, DSC, XRD, and FTIR analysis were used to characterize them.

### A. Dynamic Mechanical Analysis (DMA)

A model Q 800 TA Instruments with tension film claw was used in order to obtain  $E'$ ;  $E''$  and  $\tan \delta$  values. The films had approximate dimensions of 10/7/0.5 mm, length/width/thickness, respectively. Frequency of 1 Hz, preload 0.15N, 4000  $\mu\text{m}$  of amplitude, and a ratio of 3  $^{\circ}\text{C}\cdot\text{min}^{-1}$  of heating and a range of 40–270  $^{\circ}\text{C}$  were typical for DMA analysis.

### B. Fourier Transform Infrared Spectroscopy (FTIR)

FTIR pellets were prepared by using mixtures of CA samples and KBr and typical parameters include 32 scans in the range of 500–4000  $\text{cm}^{-1}$ . The equipment used was Nicolet IR200.

### C. Differential Scanning Calorimetry (DSC)

The differential scanning calorimeter was used to examine the thermal property of the CA samples in a temperature range of 25–300  $^{\circ}\text{C}$ . Approximately, 10 mg of the CA samples biodegradation were used. The measurements were performed in a pan Al, pierced lid in the  $\text{N}_2$  atmosphere (flow rate of 50 ml/min) at a heating rate of 5  $^{\circ}\text{C}/\text{min}$ . The results were recorded and analyzed.

### D. X-Ray Diffraction Analysis (XRD)

A diffractometer was used with a goniometer speed of 2/min, in the range of 7–70 $^{\circ}$  (2 $\theta$ ) iron pipe.

## III. RESULTS AND DISCUSSION

### A. Simulated Soil

Fig. 1 shows the containers in which the samples were buried. The fungal growth can be observed, which was expected, because it is organic matter, due to the manure added to middle of composting.

Vagner Botaro is with the Federal University of São Carlos (UFSCar), Brazil (e-mail: vagnerbotaro@gmail.com).



Fig. 1 Composting soil

Animal manure herbivores, such as horse, feature significant amount of microorganisms capable of produce cellulase, enzyme responsible for the hydrolysis of cellulosic materials, since they need the same for digestion. The cellulase is produced by a range of microorganisms, including anaerobic bacteria (*Clostridium*, *Rominooccus*, etc.), aerobic (*Cellulomonas*, *Thermobifida*, etc.), actinomycetes (*Streptomyces*), filamentous fungi (*Trichoderma*, *Bulgaria*, *Helotium*, *Poria*, *Aspergillus*, etc.), plants (*Fragaria*) and animals (mollusks and insects). Degradation by the cellulase enzyme is formed by a cellulolytic complex composed of endo- $\beta$ -1,4-glycanases, cellobiohydrolases and  $\beta$ -glycosities that act in synergism [8].

#### B. X-Ray Diffraction Analysis (XRD) Results

Fig. 2 shows the results of the x-ray diffraction for CA and biodegraded samples. Crystallinity index (CI) was calculated by the method Ruland-Vonk [9]. This method is based on the relation between the areas of crystalline domains with the total area of the diffractogram (1):

$$CI = \left( \frac{Sc}{St} \right) \times 100 \quad (1)$$

where Sc is the area of the field lens, and St is the area of total dominance.

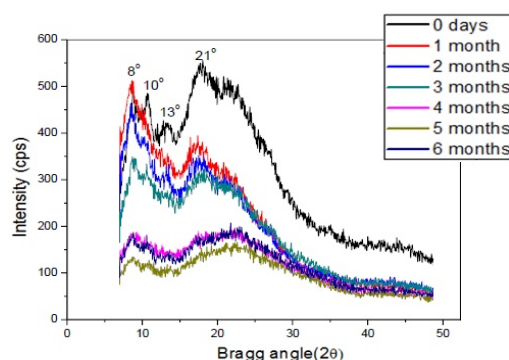


Fig. 2 X-ray diffraction results

It was observed that, as the CA underwent biodegradation, the crystalline character was improved. A typically interesting behavior can be described for the peak  $2\theta=13^\circ$ . Initially this peak is intense and visible for CA and it decreases progressively until disappearing completely in the final stages of degradation time. The literature describes the amorphous halo in  $2\theta=20^\circ$  approximately which is characteristic for semi-

crystalline CA [10]. Fig. 2 shows a decrease of this peak during degradation. On the other hand, the peak  $2-\theta = 8^\circ$ , characteristic of crystalline part remains present until the final stages of the process of biodegradation [11]. Table I relates the CI of the biodegradable samples:

TABLE I  
 CRYSTALLINITY INDEX

Time	Crystal area	Amorphous area	CI
day0	446.6	1474.0	23%
month1	328.7	515.2	38%
month2	268.8	638.0	34%
month3	281.2	723.1	28%
month4	235.8	758.8	23%
month5	140.0	616.9	19%
month6	1118.0	3809.0	22%

It can be observed in the first month of biodegradation that there was an increase in the CI, going from 23% (CA) to 38%. In general, when compared crystalline regions with amorphous ones of a polymer system, the latter are less compacted, less organized and more easily attacked, for example by microbiological in simulated soils [8]. In the following months, the index of crystallinity decreased, reaching 19% in the fifth month. As mentioned above, in the topic on polymeric biodegradation, cellulose is readily hydrolyzed by the enzyme cellulase. This enzyme is produced by microorganisms present in the feces of herbivorous animals, such as horse, which was used to prepare the simulated soil. It is expected that the substrate has a cellulase enzyme, once the presence of fungi has been observed (Fig. 1). Decrease of crystalline regions is linked to the presence of the enzyme cellulase that degrades the regions where the hydroxyls are present, regions of greater organization [12].

In the last month of biodegradation, the CI increased from 19% to 22%. The conclusion is that, in this phase of degradation, the amorphous regions are more prone to biodegradation, and therefore, there is increased crystallinity.

In calculations of mass loss biodegradation, there were no significant changes in the acetate samples with DS 2.5. However, with the results of XRD, it was verified that there was biodegradation, since the CA had a morphological change.

#### C. Differential Scanning Calorimetry (DSC) Results

DSC technique was used to evaluate the thermal behavior of the samples of CA, with DS 2.5, which were degraded at each test time. Fig. 3 shows the curves obtained in the DSC test of the biodegradable samples. The assay was performed with heating from 25 °C to about 300 °C. The first thermal event corresponds to the endothermic peak of water desorption. This is due to the presence of residual moisture in the polymer, or the presence of volatile solvents. With biodegradation time, this peak became less and less expressive. Other endothermic peaks are of glass transition and melting, respectively (Table II).

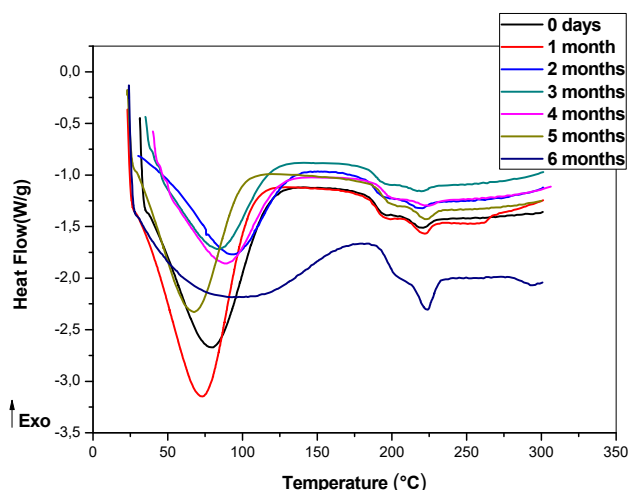


Fig. 3 DSC results

TABLE II  
DSC RESULTS

Time	T <sub>m</sub> (°C)	ΔH melting (J/g)	Desorption (°C)	ΔH Desorption (J/g)	Midpoint T <sub>g</sub> (°C)	ΔCpT <sub>g</sub> (J/g °C)
day 0	248.5	0.943	85.5	109.0	224.4	0.315
month 1	221.1	1.392	79.4	87.6	188.7	0.279
month 2	222.0	1.327	73.4	87.6	189.6	0.206
month 3	220.6	0.848	94.3	59.7	187.6	0.261
month 4	219.6	0.770	82.9	62.1	190.7	0.223
month 5	223.5	1.402	67.6	65.2	192.9	0.187
month 6	223.9	3.084	96.1	47.8	196.5	0.238

Table II lists all the results obtained by the DSC curve. Enthalpy of melting, ΔH melting (J/g), is indicative of the morphology of the polymer. Increase in this value characterizes the greater interaction of the chains, which as a consequence, requires higher energies for chain mobility, which also characterizes the fusion. As shown in Table II, a tendency to increase enthalpy (ΔH melting) can be observed for the samples that remained for a longer time in the simulated soil. The melting enthalpy values are related in an expected manner to the obtained crystallinity values (Table I). In this sense, there is a tendency for more crystalline samples which have a higher melting enthalpy values. The presence of highly compacted crystalline regions with a large number of intermolecular linkages as hydrogen ones makes it difficult to separate the chains and consequently an increases the fusion enthalpies.

#### D. Dynamic Mechanical Analysis (DMA) Results

With the dynamic-mechanical thermal assay, it is possible to evaluate changes of molecular relaxations that occur in polymer materials over a wide temperature range, which allows estimating molecular parameters and mechanical properties of the polymer. Storage module (E') corresponds to the elastic response and the more rigid the material, the larger its storage module. Loss modulus (E'') corresponds to the viscous response, the greater the loss of material modulus, and the greater its ability to dissipate mechanical energy [13]. Table III shows the results of the DMA test.

TABLE III  
RESULTS DMA

Time	E' ~ 200°C (MPa)	E'' ~ 200°C (MPa)	T <sub>g</sub> (°C)
day0	5.69 ± 0.73	4.39 ± 0.39	200.44 ± 0.40
month1	6.92 ± 1.9	3.77 ± 0.11	208.71 ± 0.70
month2	7.43 ± 1.16	3.43 ± 0.35	208.81 ± 1.08
month3	8.19 ± 0.56	2.55 ± 0.12	208.98 ± 0.42
month4	10.69 ± 0.76	2.42 ± 0.10	208.76 ± 0.63
month5	12.45 ± 0.85	2.39 ± 0.10	208.83 ± 0.66
month6	15.32 ± 0.69	2.34 ± 0.20	209.27 ± 1.00

In Figs. 4 (A) and (B) are presented storage modulus and loss modulus, respectively, as a function of temperature.

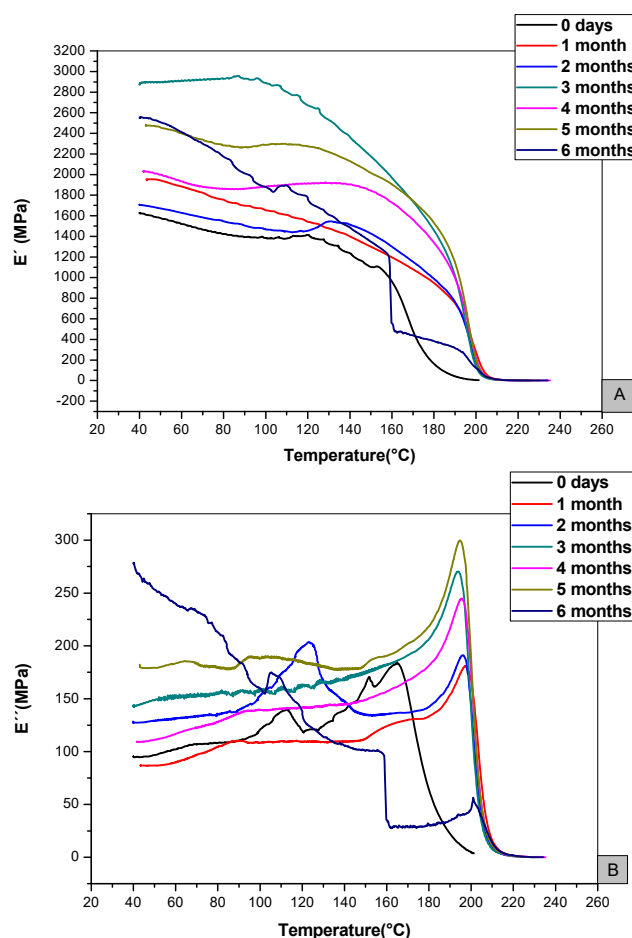


Fig. 4 DMA results (A) E' x T (B) E'' x T

By the analysis of DMA, it was possible to conclude that, as the AC is biodegraded, its mechanical properties were altered because the storage module that increased with biodegradation and the loss modulus decreased (Table III). In the simulated soil, the presence of fungi was observed, which proves organic matter essential for CA biodegradation. In general, by analyzing the dynamic-mechanical thermal behavior of the CA samples, the conclusion is that the amorphous region of the polymer is the first to be biodegraded, resulting in more crystalline regions, as observed in the results of DRX. Results showed a more rigid behavior of biodegradable samples, with

larger elastic moduli, Tg (Fig. 5) and storage module than CA without biodegradation.

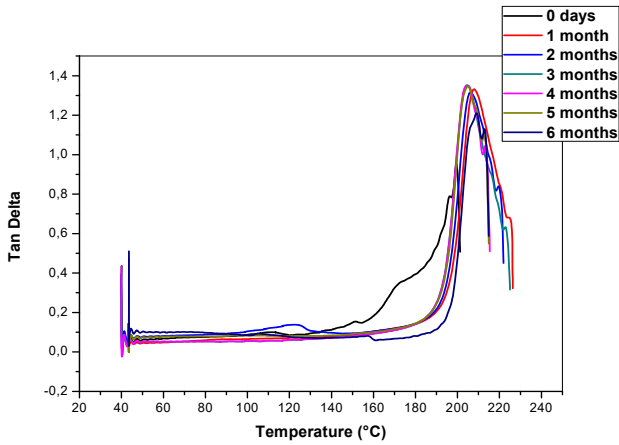


Fig. 5 Tan Delta

Loss modulus was smaller in biodegradable samples, since the ability to dissipate energy in more crystalline matter is lower. Storage Module ( $E'$ ) e Loss Module ( $E''$ ) and tan delta

modules are directly related to structure, molar mass and composition. In this way, everything restricts the movement of the chains which increases  $E'$  and decreases  $E''$ .

#### E. Fourier Transform Infrared Spectroscopy (FTIR) Results

FTIR technique was used to evaluate the characteristic bands of CA after biodegradation. Fig. 6 shows the spectrum of samples of 0 days, 2, 4 and 6 months. We chose these four because they showed the most significant changes in relation to the other samples. Spectra were amplified at wavelengths between 2000 and 500  $\text{cm}^{-1}$  for better visualization of the characteristic bands of CA. We can observe a decrease in the band at 1750  $\text{cm}^{-1}$ , referring to the carbonyl stretch of ester [14]. This is the band that characterizes CA. The decrease of this band can be observed, and comparing to the other results (DMA, DRX and DSC), it was concluded that acetyl groups were degraded. By the DSC analysis, it was possible to observe the enthalpy of water desorption which was decreasing with the biodegradation. This result was evidenced by the decrease of the band in 1645  $\text{cm}^{-1}$ , referring to the deformation of the water molecule.

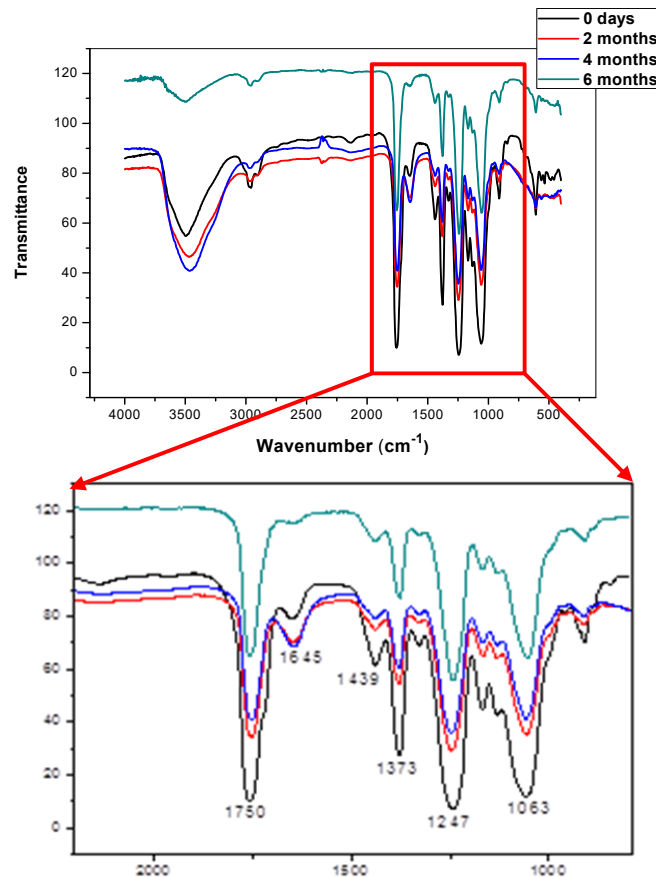


Fig. 6 FTIR results

#### IV. CONCLUSION

In the simulated soil for composting, the presence of fungi was observed, which proves organic matter essential for the

biodegradation of CA. In general, by analyzing the dynamic-mechanical thermal behavior of the CA samples, it is concluded that the amorphous region of the polymer is the

first to be biodegraded, resulting in more crystalline regions, as observed in the results of DRX. Results showed a more rigid behavior of biodegradable samples, with larger elastic moduli, Tg and storage modulus than CA without biodegradation. Loss modulus was lower in biodegradable samples, since the ability to dissipate energy in more crystalline matter is lower.

#### ACKNOWLEDGMENT

JP Project 2008-00835 FAPESP, CNPq and Capes.

#### REFERENCES

- [1] H. O. Ghareeb et al, "Molar mass characterization of cellulose acetates over a wide range of high DS by size exclusion chromatography with multi-angle laser light scattering detection" in *Carbohydrate Polymers*, 2012, v. 88, n. 1, p. 96–102.
- [2] C.C Lin; K. S. Anseth. "The Biodegradation of Biodegradable Polymeric Biomaterials. In: LEMONS, B. D. R. S. H. J. S. E. "in *Biomaterials Science (Third Edition)*. (S. 1.): Academic Press, 2013. p. 716–728.
- [3] R. L. Crawford, "Biodegradation: Principles, Scope, and Technologies. In: MOO-YOUNG, M. (Org.)" in *Comprehensive Biotechnology (Second Edition)*. Burlington: Academic Press, 2011. p. 3–13.
- [4] S. S. Brum; et al, "Synthesis of cellulose acetate from the bean straw using N-bromosuccinimide (NBS) as catalyst" in *Polímeros*, 2012, v. 22, n. 5, p. 447–452.
- [5] A. M. Senna; K. M. Novack; V. R. Botaro, "Synthesis and characterization of hydrogels from cellulose acetate by esterification crosslinking with EDTA dianhydride" in *Carbohydrate Polymers*, 2014, v. 114, p. 260–268.
- [6] S. M. M. Franchetti; J. C. Marconato, "Biodegradable polymers - a partial way for decreasing the amount of plastic waste" in *Química Nova*, 2006, v. 29, n. 4, p. 811–816.
- [7] M. A. G. Bardi; D. S. Rosa, "Avaliação da Biodegradação em Solo Simulado De Poli (Caprolactona), Acetato De Celulose E Suas Blendas" in *Revista Brasileira de Aplicações de Vácuo*, 2007, v. 26, n. 1, pp. 43–47.
- [8] C. Florencio, "Microrganismos Produtores de celulases: seleção de isolamento de *Trichoderma spp.*" *São Carlos*, 83, 2007.
- [9] K. Karimi; M. J. Taherzadeh, "A critical review of analytical methods in pretreatment of lignocelluloses: Composition, imaging, and crystallinity" in *Bioresource Technology*, 2016, 200, pp. 1008-1018.
- [10] Cerqueira, D. A. *et al.* 1H-NMR characterization of cellulose acetate obtained from sugarcane bagasse. *Polímeros*, v. 20, n. 2, p. 85–91, jun. 2010.
- [11] Wan Daud, W. R.; Djuned, F. M. Cellulose acetate from oil palm empty fruit bunch via a one step heterogeneous acetylation. *Carbohydrate Polymers*, v. 132, p. 252–260, 5 nov. 2015.
- [12] G. J. M. Fachine, "Biodegradable polymers - a partial way for decreasing the amount of plastic waste" in *Química Nova*, v. 29, n. 4, 2006, pp. 811–816.
- [13] R. R. M. de Freitas; A. M. Senna; V. R. Botaro, "Influence of degree of substitution on thermal dynamic mechanical and physicochemical properties of cellulose acetate" in *Industrial Crops & Products*, 2017, 109, pp 452–458.
- [14] R. M. Silverstein; G. C. Bassler; T.C. Morrill, "Carboxylic acid and amines" in *Spectrom. Identif. Org. Comp*, 2005, 7, 96–102.